BIOPHYSICS AND BIOCHEMISTRY

Fourier Analysis of Human Finger Bioimpedance Variances

A. V. Nesterov, I. Yu. Gavrilov, L. Ya. Selector, I. S. Mudraya*, and S. V. Revenko

Translated from *Byulleten' Eksperimental'noi Biologii i Meditsiny*, Vol. 150, No. 7, pp. 31-37, July 2010
Original article submitted November 20, 2009

Fourier analysis was employed to determine the amplitudes of spectrum components of small variations of electrical resistance (bioimpedance) in human finger recorded using an original hardware-software complex. It revealed periodic bioimpedance oscillations at the frequencies of heartbeats, respiration, and Mayer wave (0.1 Hz). These periodic variations were observed under normal conditions and during circulation arrest in the arm. It is concluded that the spectrum peaks of bioimpedance variations in the phalanx of human finger reflect periodic blood pressure changes in the major vessels and rhythmic neural control of the regional vascular tone. During normal blood flow, the greatest amplitude of rhythmic changes in bioimpedance was observed at the heart rate; it surpassed by an order of magnitude the amplitudes of respiratory oscillations and Mayer wave. In contrast, the largest amplitude of rhythmical changes of the impedance during circulation arrest corresponded to the oscillations at respiration rate, while the amplitude of variations at the heart rate was the smallest. Under circulation arrest, the maximum frequency of bioimpedance variations was approximately 1.4 Hz (the third respiratory harmonic), which indicates the upper limit of frequency range of neural modulation of vascular tone in human finger. During normal respiration and circulation, two side cardiac peaks were revealed in bioimpedance amplitude spectrum, whose amplitude reflected the depth of the respiratory amplitude modulation of pumping action of the heart. During normal breathing, the second and the third harmonics of the cardiac bioimpedance variations were split reflecting respiratory frequency modulation of the heart rate.

Key Words: *bioimpedance variations; Fourier analysis; vascular tone; cardiorespiratory modulation; Mayer wave*

Measurement of impedance (bioimpedance) of biological tissues is a routine electrophysiological method used for evaluation of regional blood flow [2, 5]. Recently, some important prerequisites arose for extension of the field of application of the impedance (rheographic) measurements in physiology due to spectacular progress in microelectronics and computer engineering, which made it possible to construct new generation rheographs characterized by better resolution, lower level of self-noise, and comprehensive system of automatic data analysis. We developed such a high-resolution rheography system, which opened up

BIOLA Scientific and Production Company, Institute of Experimental Cardiology, Russian Cardiology Research-and-Production Complex, Federal Agency for Health Care and Social Development; *Department of Experimental Modeling of Urological Diseases, Research Institute of Urology, Federal Agency for Health Care and Social Development, Moscow, Russia. ***Address for correspondence:*** s_revenko@mail.ru. S. V. Revenko

0007-4888/10/1501-0026

possibilities to examine the fine structure of rheograms and small variations of bioimpedance that looks like a "noise" in the records, but in reality indicate small and regular changes in bioimpedance under the effect of various factors. These changes could be produced not only by variations of blood pressure in major vessels, but also by the periodic changes of vascular tone induced mainly by rhythmic neurogenic activity. Theoretically, such rhythmic oscillations could be detected with a high-resolution impedance converter and Fourier analysis of bioimpedance variations. Our aim was to examine this possibility.

MATERIALS AND METHODS

The study was carried out with the help of an original hardware-software system based on high-resolution low-noise impedance converter capable of recording not only large-scale changes in bioimpedance caused by pulsatile variations of blood pressure, but also its small oscillations of various genesis. This system was developed on the basis on modern low-noise microchips (Fig. 1, *a*). The resolving power of the total (basic) impedance channel was 50 mΩ in the range of 0-1000 Ω. The broad impedance range of this channel made it possible to follow the mean value of bioimpedance during different manipulations, *e.g.* those that caused redistribution of interstitial fluid and blood in finger phalanx after arresting or resuming circulation in the arm. The resolving power of the alternating impedance channel was 250 μΩ in the range of ±4 Ω. This range was rather wide, and under the steady-state conditions, it surpassed the amplitude of bioimpedance oscillations in human finger by an order of magnitude. Thus, the developed rheography system was characterized by a high accuracy and a wide range of measurements of the total and alternating impedance values.

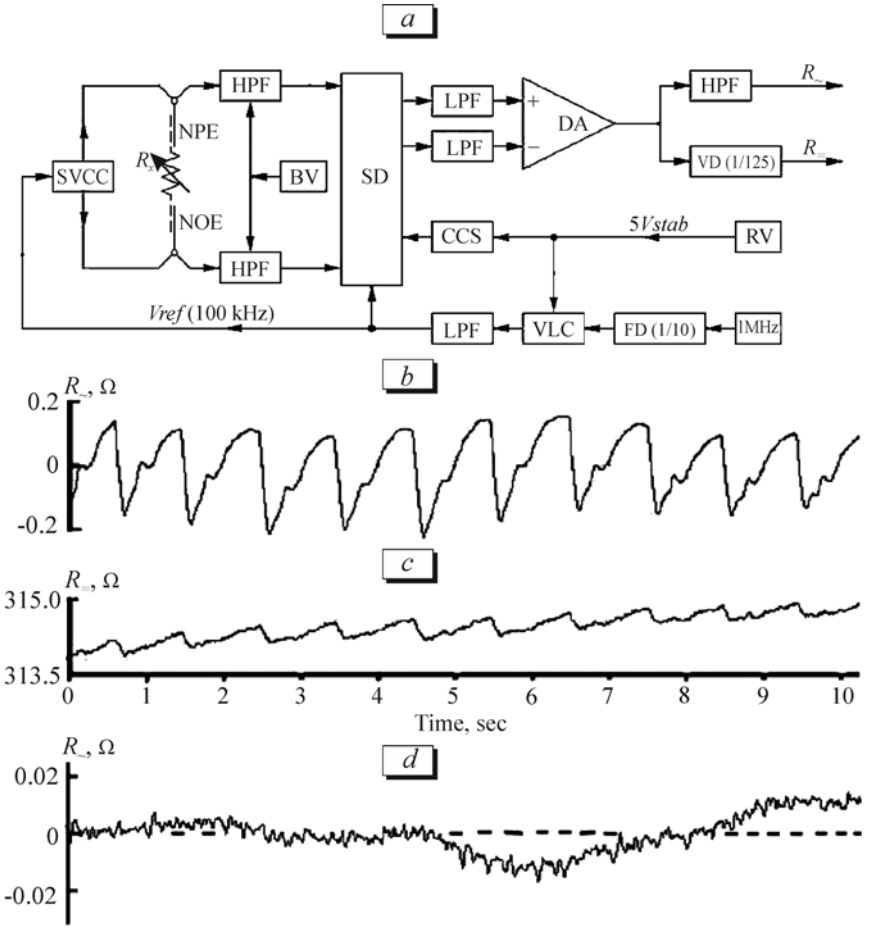

Fig. 1. Structural layout of impedance converter (rheograph, *a*) and bioimpedance components (*b-d*). *a*) SVCC, symmetrical voltage-current converter; R_x, bioimpedance; NPE, non-polarizing electrode; HPF, high-pass filter; LPF, low-pass filter; BV, bias voltage; SD, synchronous detector; CCS, constant current source; DA, differential amplifier; VLC, voltage level changer; VD, voltage divider; RV, reference voltage; FD, frequency divider; 5Vstab, stabilized voltage; V_{ref}, reference meander; $R_=$, total (basic) impedance; $R_\sim$, alternating impedance component; *b*) alternating impedance component of the proximal phalanx of the middle human finger under the normal circulation; *c*) total impedance in the same (*b*) measurement; *d*) alternating impedance component during circulation arrest in the arm. The dash line shows zero level. Frequency band 0.1-25.0 Hz.

High resolution of the impedance converter resulted from the use of a stabilized generator of alternating current with an AD780 precise voltage source (Fig. 1, *a*). The signal of this generator was fed to symmetrical voltage-current converter with integrating compensators of imbalance between the constant current components in the output currents. The probe current with a frequency of 100 kHz and an amplitude of 2 mA was applied to examined object R_x; the signal from this object was fed to a biased-output differential amplifier and then to synchronous detector MC1496. The differential outputs of this detector were fed to a low-noise differential amplifier INA128. The output of this chip (total or "basic" resistance, $R_=$) was directed to the output connector of the device via a 1:125 divider to match with the input of original analog-to-digital converter PPSh-04. The output signal was also fed to a two-pole high-pass filter with a cut frequency of 0.05 Hz and then to an input of PPSh-04 converter to record the alternating impedance component $R_\sim$.

The original 4-channel converter PPSh-04 digitized the signals at the sampling rate of 16 kHz in each channel. The first on-board microprocessor decimated the digitized signals to the rate of 160 Hz sufficient to record the changes of bioimpedance. The decimation algorithm included a cascade low-pass finite impulse response filtering to eliminate signal distortion and to optimize the work of the microprocessor. The digitized signals were passed across a galvanic isolator to PC via an USB port under the control of the second on-board microprocessor in PPSh-04.

The signals fed to PC (basic impedance $R_=$ and alternating impedance component $R_\sim$) were filtered with two-pole Bessel filter. As a rule, the low-cut frequency in the alternating impedance channel was set at 0.08 Hz. In both basic and alternating impedance channels, the high-cut frequency was set at 15 Hz. In addition, a notch filter was used to eliminate the power-supply noise at 50 Hz.

To perform fast Fourier transform, the impedance record was cut into segments of certain length ranging from 2^8 to 2^{16} data points to obtain the spectra with various frequency resolution. The spectra were calculated with the Hanning window. In most cases, the number of data points in a segment was 4096 corresponding to the length of the record of 25.6 sec. In experimental records, the chosen fragments contained no artifacts caused by the involuntary movements. Such fragments included 1 to 4 segments of the above length. The amplitude spectra of individual segments in the selected fragment of experimental record were averaged. The result of Fourier transform was plotted as a dependence of amplitude of the periodic bioimpedance components on frequency.

The impedance converter was connected to the proximal phalanx of the middle human finger (n=14, Fig. 1, *a*) by bipolar non-polarizing Ag/AgCl electrodes made of silver wire 0.4 mm in diameter. The use of such electrodes was necessary in order to diminish the low-frequency electrical noise during measurements of small bioimpedance variations. The electrodes of other types made of stainless steel, platinum, or silver-plated copper wire generated greater (by several times) low-frequency electric noise within the frequency range of 0.02-0.2 Hz. The electrodes were covered with the gauze bandages soaked in physiological saline. To damp mechanical vibrations caused by the heart and lungs, the arm with mounted electrodes was placed on a massive support. In experiments with circulation arrest in the arm, a pneumatic cuff was placed on the shoulder. The pressure in the cuff was controlled with a manometer. To ensure circulation arrest in the arm, this pressure was higher than the systolic blood pressure by more than two times.

RESULTS

The developed high-resolution rheography system can be employed to examine the fine structure of the rheograms, *e.g.* that of the venous system [2]. The specific venous spike is clearly seen on the upward edges in rheograms (Fig. 1, *b*). The plots in Fig. 1, *b*, *d* show the changes of bioimpedance with time (*the time-domain analysis*). The cause of bioimpedance changes is attributed to the changes in filling of the blood vessels due to the pumping action of the heart and the changes in vascular tone [2,5].

Important information can be obtained from presentation of the periodic variations of bioimpedance in dependence on frequency (*the frequency-domain analysis*) with the use of Fourier transform resulting in the plots showing the dependence of amplitude of periodic impedance variation on frequency (Fig. 2). Peak 1 was observed in the frequency range of 0.1-0.2 Hz. The periodic oscillations of arterial pressure in this range (about 0.1 Hz) are termed as Mayer wave [6], so the corresponding spectrum peak of bioimpedance variations is defined here as "Mayer peak". Peaks 2 and 3 were observed at the frequencies of respiration and heartbeat, respectively. Spectrum peaks 3, 3'', 3''', and 3'''' situated at multiple frequencies represent the first (fundamental) and the second, third, and fourth harmonics of pulsatile (cardiac) bioimpedance variations. The height of a cardiac harmonic decreased with its number. The presence of several harmonics in bioimpedance spectrum reflects the fact that the periodic filling of the blood vessels in finger at the pulse rate is not a strict sinusoidal process, which can be directly seen in the shape of the rheograms (Fig. 1, *b*). The

availability of several harmonics should be taken into account when evaluating the contribution of a periodic process into the total variations of bioimpedance.

In all experiments, the fundamental cardiac peak and its higher harmonics were escorted by side (left and right) peaks (Figs. 2 and 3). These side peaks were placed symmetrically near the fundamental cardiac peak and its harmonics, the frequency distance between the central and any side peak being equal to the respiration rate. This observation motivated us to compare the bioimpedance variation spectra under normal conditions and during expiratory delay (Fig. 2, *b*, *c*). Evidently, breath-holding eliminated not only fundamental respiratory peak 2 in the bioimpedance variation spectrum, but also all side cardiac peaks. Thus, these side peaks are related to respiratory activity.

The trident spectrum structure with a central peak and two smaller symmetrical side peaks is well known in physics and electronics [1]. This structure corresponds to a harmonic (sinusoidal) process with constant amplitude going on at the frequency of the central peak, which is modulated in amplitude by another harmonic process going on at a lower frequency equal to the distance between the central peak and any of the side peaks. Most probably, the trident spectrum structure of peaks 3, 3L, and 3R (Figs. 2, *a*; 3, *a*) reflects the amplitude modulation of the heartbeat force by respiratory activity. The ratio of the height of the side peaks to that of the central peak corresponds to the degree ("depth") of amplitude modulation. Thus, this ratio can quantitatively assess interaction between the cardiac and respiratory systems [3,8].

Figure 2, *b* shows a specific feature of the second, third, and fourth cardiac harmonics observed in some cases: the corresponding peaks were "dual" with the characteristic notch (incisure). In Fourier transform, the distance between the humps of dual peaks increases with increasing the harmonic number, which suggests the dual structure of the fundamental cardiac peak as well, where the humps "merged" due to insufficient resolution of Fourier transform in these experiments. Respiratory arrest eliminated "splitting" of the second and third cardiac harmonics (Fig. 2, *c*). This observation substantiates the hypothesis that the dual structure of the cardiac peaks results from frequency modulation of the cardiac work by respiratory activity. The cardiac rhythm is known to depend on the respiratory phases; it changes in time with the respiratory excursions [3,8]. The degree of such frequency modulation can be assessed by the width of the gap between both humps in cardiac harmonics. It is noteworthy that in some cases there was no splitting in the cardiac peaks (Fig. 2, *a*). To improve the accuracy in assessment of this mode of modulation, pronouncedly longer records are needed than used in this experiment (25.6 sec). A special study will be carried out on the fine structure of the cardiac harmonics in the bioimpedance amplitude spectrum.

Taken into consideration the possibility of changes in filling of finger vessels not only due to pulsatile oscillation of the arterial pressure, but also due to alterations in vascular tone resulting from various reasons (neural included), we measured and compared the bioimpedance spectra under normal (Fig. 3, *a*) and arrested (Fig. 3, *b*) circulation in the arm. Such circulatory arrest made it possible to examine the pe-

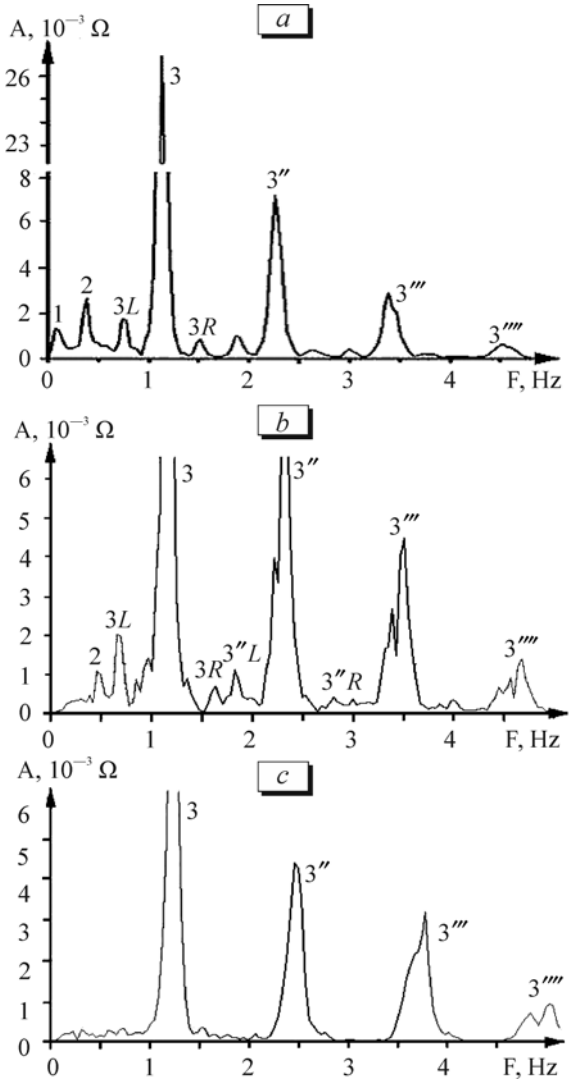

Fig. 2. Panoramic amplitude spectra of human finger bioimpedance with the major periodic components of bioimpedance variations and the harmonics of cardiac peak. *a*) *1*, Mayer peak; *2*, respiratory peak; *3*, fundamental cardiac peak. The strokes mark the harmonics of pulsatile oscillations of bioimpedance. *3L* and *3R*, the left and right side cardiac peaks, respectively. 3''L and 3''R are the similar side peaks of the second pulsatile harmonic. Frequency band 0.08-15.0 Hz. *b*, *c*) Bioimpedance amplitude spectrum under normal conditions (*b*) and during expiratory delay (*c*). Frequency band 0.3-15.0 Hz.

riodic changes of bioimpedance in the phalanx unrelated to the changes of blood pressure in the major vessels. Under these conditions, the periodic changes of phalanx bioimpedance could be produced either by rhythmic neurogenic vasomotor stimulation or by intrinsic periodic spontaneous vasomotions. The latter are characterized by a broad range at the low frequencies of 0.008-0.110 Hz [4].

Figure 3, *b* shows in an augmented scale the amplitude spectrum of phalanx bioimpedance variations during arrested circulation. The very presence of the peaks in this spectrum is an important observation, although they were lower than the analogous peaks recorded under normal circulation. This observation indicates the existence of rhythmic changes in the filling of blood vessels that are deprived of hydromechanical connection with the heart. These peaks were narrow; they were observed at Mayer frequency (peak 1), respiration frequency (peak 2), and the heart rate (peak 3). The narrow shape of the peaks attests to stability of the rate of the rhythmic changes in bioimpedance during arrested circulation. Probably, peaks 2 and 3 reflect periodic activity in vasomotor nerves at the frequencies of respiration and cardiac pulsation, respectively. The narrow shape of peak 1 testifies against the hypothesis that it results from spontaneous vasomotions. Seemingly, this peak also originates from neurogenic vasomotor activity. The expiratory delay against the background of arrested circulation eliminated all spectrum peaks except the Mayer peak (Fig. 3, *c*). The magnitude of other part of the spectrum (F>0.3 Hz) was approximately 2-fold greater than that of the impedance spectrum of two non-polarizing Ag/AgCl electrodes immersed into physiological saline at a distance of 1 cm from each other (Fig. 3, *d*). It cannot be excluded that approximately uniform bioimpedance spectrum at frequencies F>0.3 Hz ("white noise" spectrum) observed during combined arrest of circulation and respiration reflects spontaneous vasomotions in the phalanx.

During circulation arrest, the height of respiratory peak 2 was several times larger than that of cardiac peak 3. Moreover, the respiratory oscillations of bioimpedance were characterized by three harmonics, while cardiac bioimpedance variations were reflected by only one (fundamental) harmonic. It is an established fact that microneurographic recording of neural activity in the nerves innervating the skeletal muscles yields predominantly bursts of spikes discharging at a pulse rate [7]. The above data indicate the existence of powerful bursts in sympathetic efferent fibers discharging at the respiration rate, or a pronounced respiratory modulation of the bursts synchronized with the heartbeats. This hypothesis can be useful in the microneurographic studies.

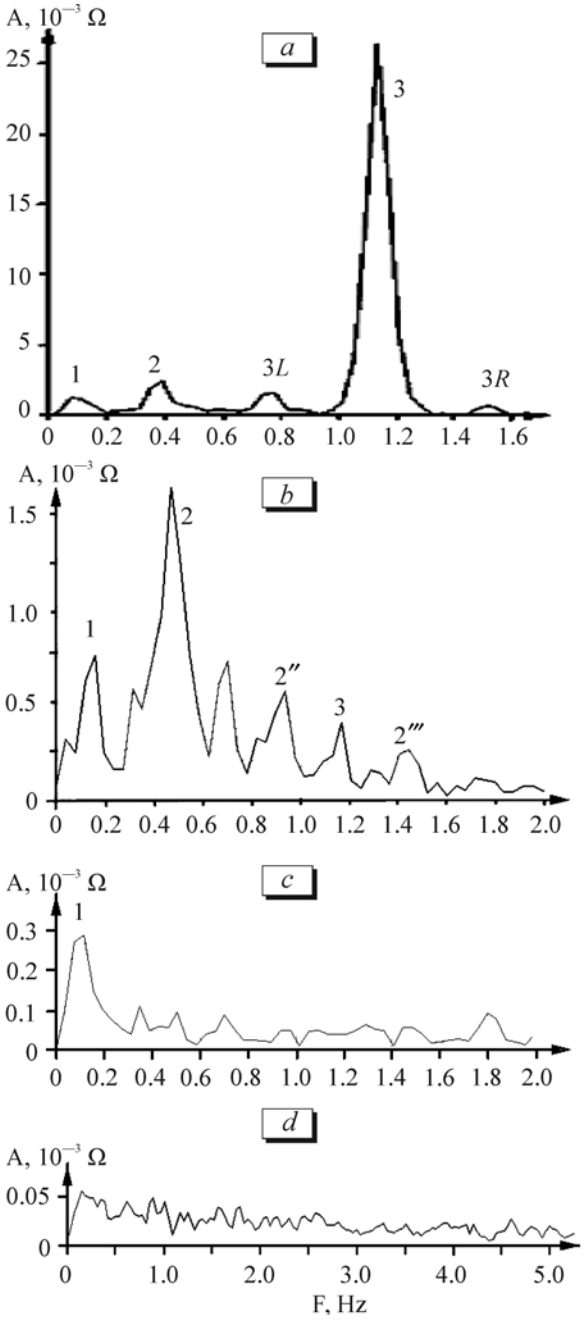

Fig. 3. Amplitude spectra of human phalanx bioimpedance under the normal conditions (*a*), during circulation arrest in the arm with normal respiration (*b*), and during circulation arrest combined with expiratory delay (*c*). *1*, Mayer peak; *2*, the fundamental respiratory peak; *2*'', the second respiratory harmonic; *2*''', the third respiratory harmonics; *3*, the fundamental cardiac (pulsatile) peak; 3L and 3R, the left and right side cardiac peaks. Frequency band 0.08-15.0 Hz. *d*) Impedance noise spectrum of a pair Ag/AgCl electrodes immersed into physiological solution with the basic resistance 40 Ω.

The pronounced decrease of the cardiac peak during circulation arrest opened the way to examine the structure of respiratory peak 2, whose height decreased less markedly under these conditions (Fig. 3, *a*, *b*). Most interesting, the second (2'') and the third (2''')

harmonics of respiratory bioimpedance variations became visible (Fig. 3, *b*). It turned out that similar to the cardiac peaks, respiratory peak 2 was accompanied with two symmetrical side peaks (Fig. 3, *b*). Under conditions of normal circulation, the side respiratory peaks were masked by far greater fundamental cardiac peak and its left side peak. Similar to above reasoning on the origin of the side cardiac peaks, it can be hypothesized that the revealed structure of three peaks reflects the amplitude modulation of respiration-driven neurogenic vasomotor activity by some slow process oscillating at the rate close to Mayer frequency. Indeed, expiratory delay produced against the background of arrested circulation suppressed not only the fundamental respiratory peak, but also his side components (Fig. 3, *b*, *c*). Although these observations favor the hypothesis on amplitude modulation of respiratory neurogenic vasomotor influences by Mayer wave, this inference cannot be considered as firmly established, because reliably recording of small side "respiratory" peaks needs further study.

Comparison of the corresponding heights of cardiac, respiratory and Mayer peaks during normal and arrested circulation (Fig. 3, *a*, *b*) shows that normally, the cardiac peak results mainly from the work of the heart and not from periodic changes of vascular tone induced by vasomotor nerves. In contrast, the major contribution to Mayer and respiratory peaks under normal circulation originates from vasomotor influences of the autonomic nervous system. Thus, the heights of Mayer and respiratory peaks during normal circulation can assess activity of regional vasomotor influences of the autonomic nervous system. The maximum frequency of bioimpedance variations under circulation arrest was approximately 1.4 Hz (the third respiratory harmonic 2''', Fig. 3, *b*), which makes it possible to evaluate the upper limit of the frequency range of neurogenic control of the vascular tone in human finger.

The considered examples of application of Fourier analysis to bioimpedance variations demonstrate that the spectrum bioimpedance analysis is a novel powerful tool to examine the regional neurogenic vasomotor influences and interaction between the cardiovascular and respiratory systems. Our preliminary experiments on rat kidneys, rat urinary bladder, human facial muscles, and human penis showed that different regions of the body are characterized by individual spectrum structure of bioimpedance variations. There are sound reasons to believe that Fourier analysis of bioimpedance variations will be a useful tool to assess activity of the nervous system in individual organs and parts of the body having autonomic innervations.

We are grateful to Prof. V. N. Burov, V. V. Ermishkin, A. R. Ibragimov, E. V. Limonov, E. V. Lukoshkova, V. P. Mokh, S. S. Nikitin, E. G. Popov, and M. V. Stranadko for the help in carrying out experiments. We are deeply grateful to Academicians N. A. Lopatkin and E. I. Chazov, to Prof. A. V. Sivkov and V. I. Kirpatovsky whose help was decisive in this study.

This work was supported by the Russian Foundation for Basic Research (grant No. 10-04-00622a).

REFERENCES

1. S. I. Baskakov, Radiotechnical Circuits and Signals [in Russian], Moscow (2005).
2. M. A. Ronkin and L. B. Ivanov, Rheography in Clinical Practice [in Russian], Moscow (1997).
3. L. Bernardi, C. Porta, A. Gabutti, et al., Auton. Neurosci., 90, Nos. 1-2, 47-56 (2001).
4. F. Christ, P. Raithel, I. B. Gartside, et al., J. Physiol., 487, Pt. 1, 259-272 (1995).
5. S. Grimnes and O. G. Martinsen, Bioimpedance and Bioelectricity Basics, San Diego, Academic Press (2000).
6. C. Julien, Cardiovasc. Res., 70, No. 1, 12-21 (2006).
7. T. Mano, S. Ivase, and S. Toma, Clin. Neurophysiol., 117, No. 11, 2357-2384 (2006).
8. E. W. Taylor, D. Jordan, and J. H. Coote, Physiol. Rev., 79, No. 3, 855-916 (1999).